# Available Transfer Capability (ATC) as Index for Transmission Network Performance – A Case Study of Nigerian 330kV Transmission Grid

Ahmad Abubakar Sadiq, Mark Ndubuka. Nwohu, and Agbachi E. Okenna

Department of Electrical/Electronic Engineering, Federal University of Technology, Minna. Nigeria.
ahmad.abubakar@futminna.edu.ng, mnnwohu@yahoo.com, euokenna@futminna.edu.ng

**Abstract:** Performance measurement of transmission system is vital to proper planning and operations of power systems in the presence of deregulation. Degree of performance is often measured by technical and financial key performance indicators (KPIs) often determined by unavailability, quality of supply and energy lost. This paper implement a novel method, Hybridized continuous repeated power flow (HCR-PF) to compute inter-area ATC and gives a method based on computed ATC to determine the transmission efficiency by measuring the transmission system transfer efficiency in terms of available transfer capability. Available Transmission Transfer Efficiency (ATTE) expresses the percentage of real power received resulting from inter-area available power transfer. The results show that HCR-PF provides a good approximate alternative to ATC computation which is validated using IEEE 30 bus test network. The Tie line (physical path) performance is obtained by calculating the required sending end quantities with specified receiving end ATC and the receiving end power circle diagram.

**Keywords:** Transmission System, Efficiency, Performance, Available Transfer Capability, Real power.

## 1. Introduction

Globally, utility companies are implementing competitive and deregulated framework of electrical supply thereby replacing traditional and centralized controlled grid structures, resulting into increase volume of bilateral transactions as well as operation and control of power systems in different ways. Deregulation may also prompt customers to buy cheap electricity from remote location. Hence, transmission grids are going to be operated closer and closer to their limits. In the structure of deregulation, generation resources are often managed and operated by independent power producers while government adequately provide the facility of economical transaction between generators and consumers [1, 2]. The transmission network delivers large volumes of electricity from generation companies to users; including the distribution companies. Electric Power transmission companies usually measure their achievements by using various types of qualitative and quantitative assessments. The quantitative indicators are commonly known as Key Performance Indicators (KPIs). Technical and financial KPIs can be used to measure the degree of achievements through monitoring of a number of performance indicators. The technical and financial KPIs may include: System Average Interruption Frequency Index (SAIF), System Average Interruption Duration Index (SAID), Energy Not Supplied (ENS), Average Interruption Time (AIT), Overhead Lines Maintenance Cost Index (OHLMCI) and Substation Maintenance Cost Index (SSMCI) [3]. Technical performance of electricity transmission system is also quantified using measures such as system unavailability, quality of supply and energy lost. Energy lost measured in MWh is a transmission system incident occurrence such as element outages [4].

In recent years, the electric power industry in Nigeria has witness increase investment in electric power generation facility in order to meet increase in demand from consumers, without a proportionate investment in transmission; coupled with the difficulties in new transmission facility (acquiring new right of ways), optimal and reliable operations of the existing

Received: July 23rd, 2013. Accepted: September 1st, 2014

transmission interconnections is sought after as an immediate solution; hence the need to assess transmission network performance for secure operation and planning as well as avoid congestion in an emerging Nigerian power sector deregulation. ATC and TTC are both indicators of transmission system performance [5].

The ability to accurately and rapidly assess the capabilities of the transmission grid is a key concept in the restructuring of the electric power industry [6]. Frequent estimation of transfer capabilities are needed to ensure that the combined effects of power transfers resulting from multilateral transactions do not cause an undue risk of transmission system overloads, equipment damage, blackouts or transmission system collapse. The Nigerian 330kV transmission grid is characterized by various constraints and limitations ranging from voltage sags and instability, system collapse, slow expansion of transmission grid and transfer capability and capacity. These can be attributed to load growth and contingencies such as line outages and simultaneous bilateral transaction [7, 8].

ATC of a transmission system is a measure of the unutilized capability of the system at a given time and depends on factors such as Load demand, generation dispatch, network topology, simultaneous transfer, and power transfer between areas and the limits imposed on the transmission network due to thermal, voltage, generator reactive power and stability limits [9]. Moreover, ATC is again the transmission limit for reserving and scheduling energy transactions in competitive electricity markets. Accurate evaluation of ATC is essential to maximize utilization of existing transmission grids while the transmission system is adequately secured [10].

Different methods have been used for transfer capability computations, this include: Repeated power flow [11, 12, 13], Continuation power flow [14, 15, 16, 17], optimal power flow [1, 11] and Sensitivity analysis [18]. In this paper, Hybridized continuous-repeated (HCR-PF) power flow is proposed by the authors and used in this paper [8, 19].

## 2. Hybridized Continous-Repeated Power Flow (HCR-PF)

To apply continuation method to power flow problem, a loading parameter must be inserted into the power flow equations to parameterize the load-flow equation [14]. A uniform power factor model is formulated and documented in [8]. The formulation by [12, 20] shows there is a close connection between optimization, continuation power flow (CPFLOW) and repeated power flow (RPF) or successive iterative load flow computation for Transfer Capability computations or determination. Inter-area ATC can be calculated by simultaneously increasing power injection and extraction at the source and sink areas respectively. CPFLOW can therefore solve the power flow equation as an optimization problem stated thus: [21, 22]

$$\max(\lambda)$$

Subject to:

$$f(x,\lambda) = 0 \tag{1}$$

$$\left|P^{i}{}_{G}\right|_{\min} \le \left|P^{i}{}_{G}\right| \le \left|P^{i}{}_{G}\right|_{\max} \tag{2}$$

$$\left|Q^{i}{}_{G}\right|_{\min} \le \left|Q^{i}{}_{G}\right| \le \left|Q^{i}{}_{G}\right|_{\max} \tag{3}$$

$$\left|V_{i}\right|_{\min} \le \left|V_{i}\right| \le \left|V_{i}\right|_{\max} \tag{4}$$

$$\left|P_{ij}\right|_{\min} \le \left|P_{ij}\right| \le \left|P_{ij}\right|_{\max} \tag{5}$$

Equation (1) is the compact power flow equation, equations (2) and (3) are the PV real and reactive power limitations, equation (4) is the bus voltage limits while equation (5) is the thermal limits of lines connecting buses.

Hybridized Continuation-Repeated Power Flow implements power transfers by increasing complex load with uniform power factor at every PQ bus in sink area with increase in real

power injection at PV buses in the source area at incremental steps up to a binding security limit, above which system security is compromised. The proposed algorithm is implemented in Power System Analysis Toolbox (PSAT) to:

1. Establish a feasible base case, by specifying generation and loading level, bus voltage magnitude and limits as well as line/transformer thermal limits.
2. Run the resulting feasible base case power flow using Newton Raphson (NR) power flow.
3. Specify transfer direction by connecting power supply bid block at all generator buses in source area and connecting power demand bid block at all load buses in sink area
4. Set up and run CPF in PSAT with specify number of points and step size control.
5. Check for limit violation in IV
6. If yes go to IV and reduced step size else increase step size in IV until the binding security limit is just removed or about to be encountered.
7. Calculate ATC using equations (6) and report ATC value and the binding limitation.

Figure 1 shows the flow chart of the proposed Hybridized Continuation-Repeated Power Flow structure.

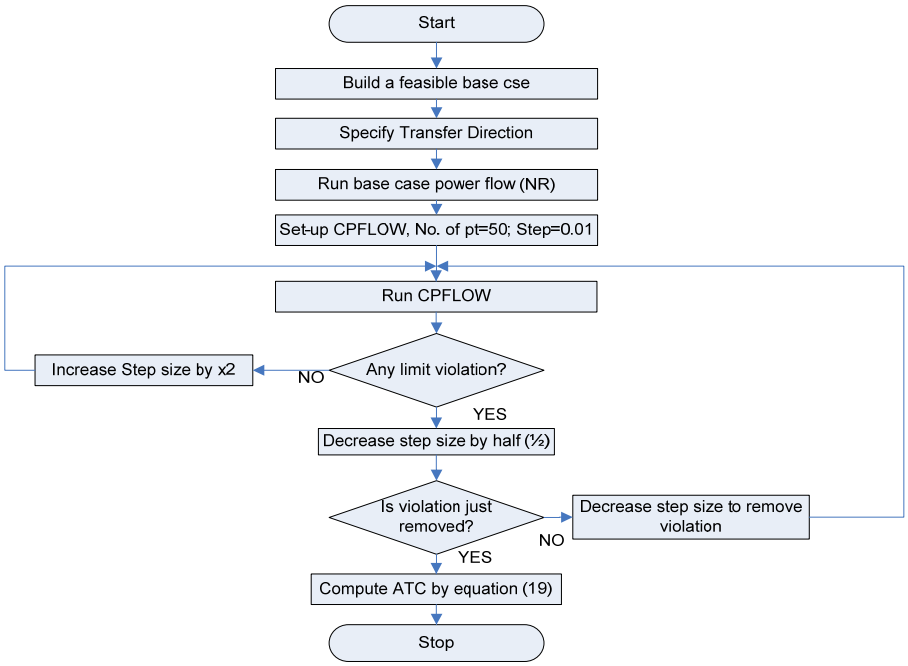


Figure 1**.** Flowchart of the proposed Hybridized Continuation-Repeated Power Flow Structure.

*Step-Size Control*

Hybridized Continuation-Repeated Power Flow (HCR-PF) like Continuation Power Flow (CPFLOW) is a procedure which employs predictor-corrector scheme in finding the solution path of reformulated sets of power flow equations that includes the loading parameter. Within the radius of convergence of the corrector, step – size control is a critical choice that affects the computational efficiency of HCR-PF. Theoretically, the step length is adapted to the shape of the path being traced; large length for flat part while small for part with high degree of curvature. The task of designing the step length is often difficult as the shape of the path to be trace is unknown beforehand. As illustrated in figure 2, the step size implementation adopted in the HCR-PF structure start with a step – size of 0.01 corresponding to a loading point A. If there is no violation (Line thermal limits, voltage magnitude and generator reactive power), HCR-PF structure increase the step size to a loading point B (0.02) and then to loading point C (0.04) where a limit violation is encountered. HCR-PF structure then reduces the step size by

half of the increment between point B (0.02) and C (0.04) to a new loading point D (0.03); should there be violation at this new point, the structure move to point E (0.025) and continues repeatedly [8].

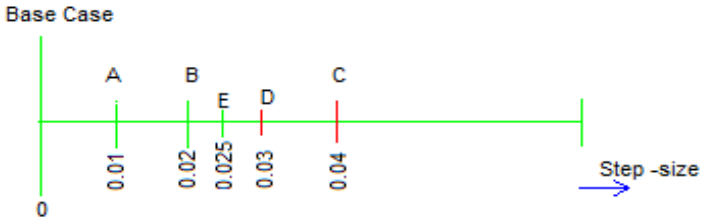


Figure 2. Step – size control implementation of HCR-PF Structure.

At the maximum loading parameter ($\lambda_{max}$), the ATC is calculated using equation (6)

$$\text{ATC} = \sum_{i \in \text{sink}} \text{P}_\text{L}^\text{i}(\lambda_{\text{max}}) - \sum_{i \in \text{sink}} \text{P}_\text{L}^{\text{i0}} \tag{6}$$

Where $P_L^i(\lambda_{\text{max}})$ is the i$^{th}$ bus real power load at maximum loading parameter in the sink (receiving) area and $P_L^{i0}$ is the same i$^{th}$ bus real power load at base case before the transfer direction. It is worthy of mention here that the i$^{th}$ bus real power load at maximum loading parameter in the source (sending) area may be used; however, the nonlinearity nature of power systems results in some real power losses. Hence, ATC obtained will be a more optimistic value as it neglect the power mismatches due to line power flows.

## 3. Transmission Line Model and Performance

A Transmission line consists of conductors running over steel towers. These lines are in-between transformation stations to evacuate generated power from power stations to major load centers. The line inter-connects all power stations forming a solid network accessible by load centers. Transmission lines are usually represented on a per phase basis by their equivalent model with appropriate circuit parameters. Line to neutral voltages and one line (phase) current are used to express the terminal voltage, thus, allow a three phase system to be reduced to its equivalent single phase. Models adopted for transmission lines and used to calculate voltage, currents, and power flows are classified based on the length of the line [23]. The three models are outlined as follows:

1. Short line model: Lines less than 80km length or voltage not more than 69KV.
2. Medium line model: Lines above 80km long but less than 250km.
3. Long line model: Lines of length 250km and longer.

A short line model is documented as follows; for a short line with a three-phase load $S_{R(3\phi)}$ connected at the end, the current received at the end is given by equation (7).

$$I_R = \frac{S^*_{R(3\phi)}}{3V^*_R} \tag{7}$$

The voltage at the sending end (8) of the transmission line has two components, the receiving end voltage and the drop component resulting from losses.

$$V_\text{S} = V_R + ZI_R \tag{8}$$

Neglecting the shunt capacitance, receiving end current becomes equal to the sending end current.

$$I_s = I_R \tag{9}$$

Figure 3 shows the two-port representation of transmission line; while equations (8) and (9) can be written in terms of the generalized ABCD constant expressed in matrix form in equations (10).

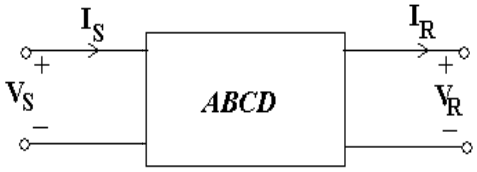


Figure 3. Two port representation of a Transmission line.

$$\begin{bmatrix} V_S \\ I_S \end{bmatrix} = \begin{bmatrix} A & B \\ C & D \end{bmatrix} \begin{bmatrix} V_R \\ I_R \end{bmatrix} \tag{10}$$

From equations (2) and (3) the ABCD constants are defined for a short line as,

A =1, B =Z, C = 0, and D = 1.

Complex power flow through a transmission line can be express in terms of both the sending and receiving end voltage magnitudes and angles and the ABCD constant [23].
Let these constant be expressed in polar form as follows,

$$\boldsymbol{A} = |\boldsymbol{A}|\angle\theta_{\boldsymbol{A}}, \mathbf{B} = |\boldsymbol{B}|\angle\theta_{\boldsymbol{B}}, \boldsymbol{V_S} = |\boldsymbol{V_S}|\angle\delta \textbf{ and } \boldsymbol{V_R} = |\boldsymbol{V_R}|\angle 0$$

where, $V_S$ and $V_R$ are the sending and receiving end voltages respectively.
From equation (10) the receiving end current is written in equation (11)

$$\boldsymbol{I_R} = \frac{|\boldsymbol{V_s}|\angle\delta - |\boldsymbol{A}|\angle\theta_{\boldsymbol{A}}|\boldsymbol{V_R}|\angle 0}{|\boldsymbol{B}|\angle\theta_{\boldsymbol{B}}} = \frac{|\boldsymbol{V_s}|}{|\boldsymbol{B}|}\angle\delta - \theta_{\boldsymbol{B}} - \frac{|\boldsymbol{A}|\boldsymbol{V_R}\|}{|\boldsymbol{B}|}\angle\theta_{\boldsymbol{A}} - \theta_{\boldsymbol{B}} \tag{11}$$

The complex power at the receiving end expressed in terms of its real and imaginary components is given in equations (12) and (13).

$$\boldsymbol{S_{R(3\Phi)}} = \boldsymbol{P_{R(3\Phi)}} + \boldsymbol{jQ_{R(3\Phi)}} = 3\boldsymbol{V_R I_R^*} \tag{12}$$

When equation (11) for $I_R$ is substituted in equation (12), equation (13) is obtained in terms of the line to neutral voltages.

$$\boldsymbol{S_{R(3\Phi)}} = 3\frac{|\boldsymbol{V_S}\|\boldsymbol{V_R}|}{|\boldsymbol{B}|}\angle(\theta_{\boldsymbol{B}} - \delta) - 3\frac{|\boldsymbol{A}\|\boldsymbol{V_R}|^2}{|\boldsymbol{B}|}\angle(\theta_{\boldsymbol{B}} - \theta_{\boldsymbol{A}}) \tag{13}$$

Generally, $Cos(\theta_B - \delta)$ and $Cos(\theta_B - \theta_A)$ in equation (13) are for the real power component while $Sin(\theta_B - \delta)$ and $Sin(\theta_B - \theta_A)$ are that of the reactive components, when expressed in trigonometry function.

Similarly, the sending end power is given by equation (14).

$$S_{S(3\phi)} = P_{S(3\phi)} + jQ_{S(3\phi)} = 3V_S I_S^* \tag{14}$$

Solving for the receiving end voltage and current in equation (10), equation (15) is obtained. From (15), $I_R$ is obtained in equation (16); noting that the π line model is a symmetrical two-port network, so that $A = D = |A| \angle \theta_A$.

$$\begin{bmatrix} V_R \\ I_R \end{bmatrix} = \begin{bmatrix} D & -B \\ -C & A \end{bmatrix} \begin{bmatrix} V_S \\ I_S \end{bmatrix} \tag{15}$$

$$I_R = \frac{|A| \angle \theta_A |V_S| \angle \delta - |V_R| \angle 0}{|B| \angle \theta_B} \tag{16}$$

With equation (16), the real and reactive power at the sending end of the line can be calculated, when equation (16) is substituted into equation (14).

The expression for real and reactive power transfer over a lossless line $(B = jX^{'}, \theta_A = 0, \theta_B = 90$ and $A = Cos\beta l)$ model is given by equation (17) and (18) respectively. Where $\beta$, $\delta$ and $l$ are the phase constant, power angle and the line length respectively.

$$P_{R(3\phi)} = \frac{|V_{S(L-L)}||V_{R(L-L)}|}{X} \sin \delta \tag{17}$$

$$Q_{R(3\phi)} = \frac{|V_{S(L-L)}||V_{R(L-L)}|}{X} \cos \delta - \frac{|V_{R(L-L)}|^2}{X} \cos \beta l \tag{18}$$

From equation (17), observe that for a given system operating at constant voltage, the real power transferred is proportional to the sine of the power angle. Theoretically, the maximum power transferred under a stable steady state operating condition will occur for $\delta = 90^o$. However, the transmission system is a network of interconnected synchronous machines; it must without loss of stability possess the ability to withstand disturbances due to sudden changes in generation, load and faults conditions. The practical operating load angle is usually limited between $35^o$ to $45^o$.

The mismatches between the sending and receiving end real and/or reactive power flows account for the line losses and expressed in equations (19) and (20).

$$P_{L(3\phi)} = P_{S(3\phi)} - P_{R(3\phi)} \tag{19}$$

$$Q_{L(3\phi)} = Q_{S(3\phi)} - Q_{R(3\phi)} \tag{20}$$

The plot of $Q_{R(3\phi)}$ versus $P_{R(3\phi)}$ for fixed line voltages and variable load angles is a circle; the locus of points obtained is called the receiving end power circle diagram. Such circles obtained with fixed receiving end voltages and varying sending end voltages are useful in the assessment of the performance characteristics of a transmission line [23].

*Transmission line Thermal Limit and Efficiency*

Power handling ability of transmission line is limited by thermal loading limit and the stability limits. Thermal limits measurement (as available in manufacturer's data) establishes the current carrying capacity of a conductor, or the maximum amount of current that can flow

through a transmission line or electrical equipment/facility over a given period (time) before a permanent damage is sustained or before public safety requirement is violated. Often express in Amperes, it is usual in Transfer Capability computation to also specify thermal limits of lines or transformers in MVA (Mega volts-amperes) or MW (Megawatts). Let the current-carrying capacity be denoted by $I_{thermal}$ and then the thermal loading of a line in VA (or MVA) is given by equation (21).

$$S_{thermal} = 3 \times V_{\phi rated} \times I_{thermal} \tag{21}$$

The transmission system efficiency of a line engaged in the transfer of power is given by equation (22)

$$\eta = \frac{P_{R(3\phi)}}{P_{S(3\phi)}} \tag{22}$$

where $P_{R(3\emptyset)}$ and $P_{S(3\emptyset)}$ are the total real power at both receiving and sending ends of the transmission line respectively.

*Available Transfer Capability as Index*

Amount of power transferable over a given line above already committed uses is a measure of the Available transfer capability, often limited by the line thermal loading and hence a measure of transmission system performance. Various transfer cases with contingency consideration to simulate the resulting effects on power flows while considering thermal, voltage and generator reactive power limits gives an in-depth measure of transmission system performance in the presence of various power transfer scenarios considered. In this paper, tie line inter-area contingencies were considered in the Nigerian 330kV transmission grid. The ratio of Available real power transfer at buying (receiving) and selling (sending) end is a measure of the transmission system efficiency for a given solved transfer case and direction. Consequently, in this paper, we introduce a novel concept to determine the transmission transfer capability efficiency by the term Available Transmission Transfer Efficiency (ATTE). Available transmission real power transfer efficiency is then defined as the ratio of the real power transfer at the receiving (buying) and sending (selling) end bus.

$$ATTE_{thermal} = \frac{P^{atc}_{R(3\phi)}}{P^{atc}_{S(3\phi)}} \times 100\% \tag{23}$$

where $ATTE_{thermal}$ is the Available Transmission Transfer efficiency, the transfer here is limited by transmission thermal loading. $ATTE_{thermal}$ is the transmission system efficiency peculiar to the specified transfer case. $P^{atc}_{R(3\emptyset)}$ and $P^{atc}_{S(3\emptyset)}$ are the real power in MW transferred to/from the buying (receiving) and selling (sending) end buses respectively.

In this paper, the Nigerian 330kV transmission grid is divided to four areas in conformity with the utility structure of Island, hence, inter-area Available transfer capability between the four identified areas are considered [19].

*Inter-Area Power Transfer*

For line performance analysis, the transfer case is modelled such that at the maximum loading parameter which gives the Available transfer capability, the load at the receiving end is the sum of the load buses which is a member of the receiving area (i.e. area2) given in equation (24).

$$P^{RA}_{L(\lambda_{\max})} = \sum_{i \in RA} P^{i}_{L(\lambda_{\max})} \tag{24}$$

Where $P_{L(\max)}^{RA}$ is the total real load of the receiving area (RA) at the maximum loading parameter $\lambda_{max}$ while $p_{L(\lambda \max)}^{i}$ is the i[th] bus real power load of the receiving area at $\lambda_{max}$.

## 4. Results and Discussion

Table 1 gives the contingency ATC values of IEEE-30 bus system, which shows the comparison between the HCR-PF and the method implemented in reference [18]. The proposed method is seen to provide a good alternative to ATC computation. In addition the last corrector step solution result of HCR-PF in Power Systems Analysis Toolbox (PSAT) environment which is obtainable in Excels identifies the limitation type and element rather than the searching techniques. Hence, as shown in table 1, the limiting line corresponding to each contingency transfer case is identified.

Figure 4 compares clearly the HCR-PF method and the approach adopted in [18]. The transaction involves bus 14 to bus 21 with various (N-1) line outages considered as contingency.

Table 1**.** Contingency ATC Values from Bus 14 to Bus 21 of IEEE-30 bus

| Bilateral Transaction | Transaction Number | Outage Line | | Limiting Line | | ATC By Hybridized C-RPF | ATC By Wu's Method |
|---|---|---|---|---|---|---|---|
| | | From | To | From | To | ATC (MW) | ATC(MW) |
| From Bus 14 To Bus 21 | 1 | 12 | 14 | 14 | 15 | 22.2 | 22.2 |
| | 2 | 12 | 15 | 14 | 15 | 13.4131 | 13.5376 |
| | 3 | 12 | 16 | 14 | 15 | 28.77 | 28.0768 |
| | 4 | 14 | 15 | 10 | 21 | 28.49 | 28.4403 |
| | 5 | 15 | 18 | 10 | 21 | 33.7824 | 33.7682 |
| | 6 | 15 | 23 | 10 | 21 | 21.227 | 21.7515 |
| | 7 | 16 | 17 | 14 | 15 | 28.3627 | 28.8257 |
| | 8 | 10 | 17 | 10 | 21 | 29.3251 | 29.4786 |
| | 9 | 18 | 19 | 10 | 21 | 33.4643 | 32.5241 |
| | 10 | 19 | 20 | 10 | 21 | 28.7402 | 28.7572 |
| | 11 | 10 | 20 | 10 | 21 | 27.5504 | 27.9273 |
| | 12 | 10 | 21 | 21 | 22 | 11.669 | 14.289 |
| | 13 | 10 | 22 | 10 | 21 | 12.0471 | 13.1917 |
| | 14 | 22 | 24 | 10 | 21 | 27.8676 | 27.8809 |
| | 15 | 23 | 24 | 10 | 21 | 24.0214 | 24.1305 |

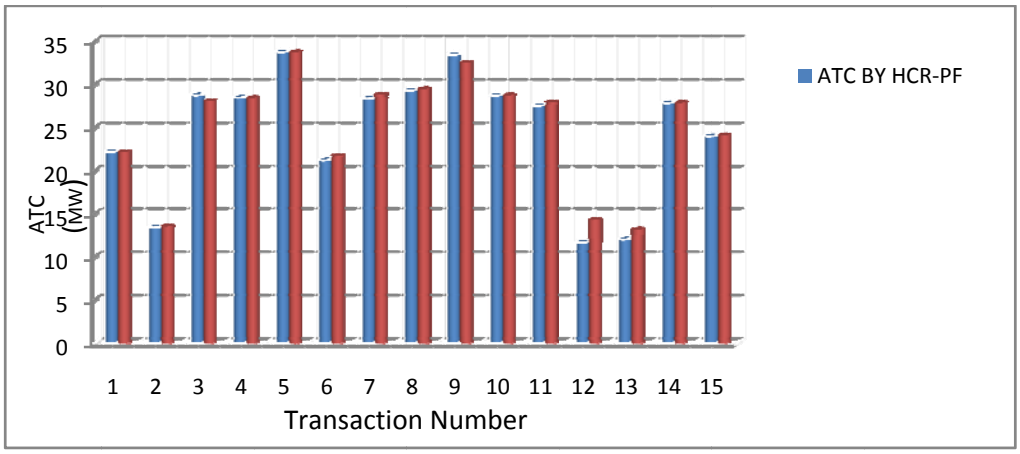


Figure 4. Comparison between HCR-PF and Wu's Method in IEEE 30 bus network for Bus 14 to bus 21 transaction.

*Bus 3 (Jebba TS) TO Bus7 (Oshogbo)*

This tie line physically connects area1 to area2 only, without any physical path from area1 to other areas. Radial nature of the grid makes this tie line critical to the entire grid. However, transactions involving other areas (area2, area3 and area4) with area1 are equally considered to adequately analyse the tie performance. The tie line is a three phase, 50Hz, 330kV transmission line of length 157km. The line parameters are R = 0.078Ω/km, C = 0.022218μF/km, L = 0.606mH/km. The line thermal rating is $I_{thermal}$ = 1360A [8]. Nominal π model is used in this paper for the tie line.

Table 2 gives the inter – area ATC computed values of Nigerian 330KV network while figure 5 depicts these ATC computed values between the four areas. It is observed that area 2 and area 4 has little or no transfer capability when compared to area 1 and area 3. As also expected, transfer capability is directional as the transfer from area 1 to area 2 is not the same as area 2 to area 1.

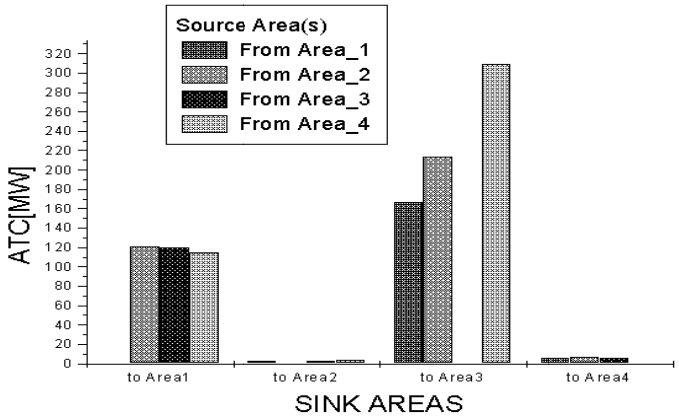


Figure 5**.** Inter – Area ATC of Nigeria Grid.

Figure 6 shows that for Area 1 (source Area) to Area 2 (Sink Area) transfer, all the source area generators (Jebba PS, Shiroro PS and Kainji PS) start at their respective base case (450MW, 490MWand 596MW) up to the transfer limitation point where the maximum loading parameter ($\lambda_{max}$) is 0.0889 corresponding to 490MW, 533MW and 640MW respectively. Figure 7 shows the increase in real power demand at the PQ buses of the sink area. All values are on 100MVA base. Figure 8 shows the tie line's additional real power flow increment up to the binding security limit for Area 1 to Area 2 transfer.

Table 2**.** Inter – Area ATC Computations of Nigerian Grid.

| **INTER - AREA TRANSFERS (MW)** | | | | | |
|---|---|---|---|---|---|
| **Source/Sink Area** | | **SOURCE AREAS** | | | |
| | | **AREA 1** | **AREA 2** | **AREA 3** | **AREA 4** |
| **SINK AREAS** | **AREA 1** | Void | 2.61 | 167.26 | 6.58 |
| | **AREA 2** | 121.43 | Void | 213.30 | 7.01 |
| | **AREA 3** | 120.00 | 3.28 | Void | 6.59 |
| | **AREA 4** | 114.69 | 4.00 | 309.56 | Void |

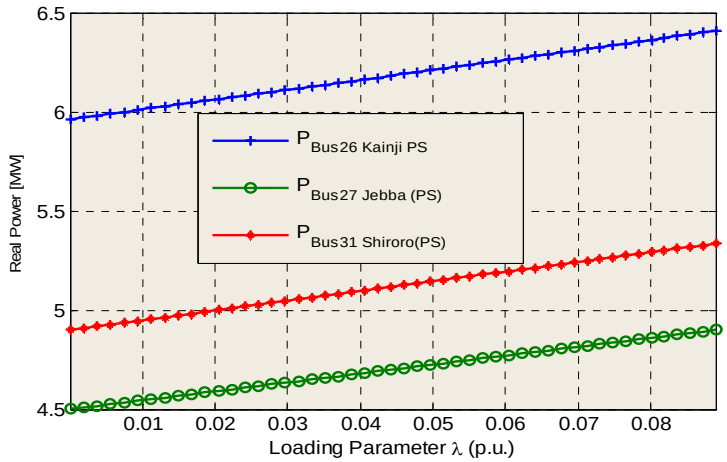


Figure 6. Increase in real power Supply at the PV buses for Area 1 to Area 2 Transfer.

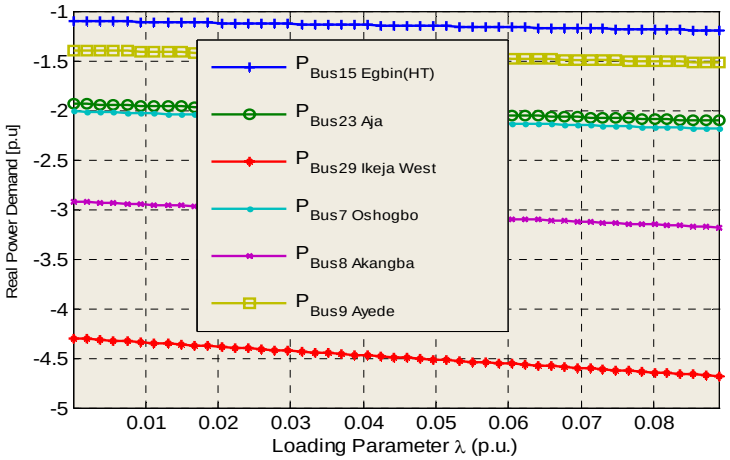


Figure 7. Increase in real power demand at the PQ buses for Area 1 to Area 2 Transfer.

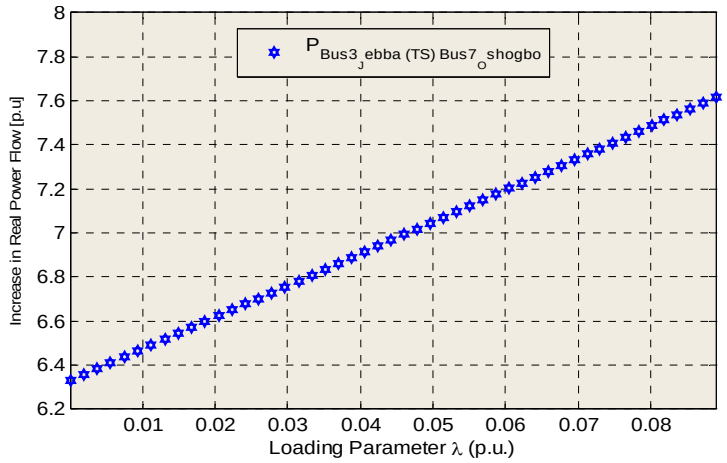


Figure 8. Increase in Line (Jebba TS to Oshogbo) Real power flow with loading parameter for Area 1 to Area 2 Transfer.

*Available Transmission Transfer Efficiency (ATTE)*

Inter-area transmission transfer efficiency of the Nigerian 330kV transmission grid was considered. Table 3 shows the Inter – Area ATTE values among the four areas of the Nigerian grid.

Table 3. Inter-area Transmission Transfer Efficiency of Nigerian grid

| **Inter-area Transmission Transfer Efficiency (%)** | | | | | |
|---|---|---|---|---|---|
| **Source/Sink Area** | | **SOURCE AREAS** | | | |
| | | **AREA 1** | **AREA 2** | **AREA 3** | **AREA 4** |
| **SINK AREAS** | **AREA 1** | Void | 93.88 | 90.89 | 91.64 |
| | **AREA 2** | 94.82 | void | 96.64 | 95.37 |
| | **AREA 3** | 99.91 | 97.91 | void | 97.05 |
| | **AREA 4** | 93.65 | 94.56 | 92.60 | void |

In Table 4 the transmission transfer efficiency of simultaneous inter-area transfer were presented. Two areas are considered as sources (sending area) among the four areas while a single sink (receiving) area different from the source areas is also chosen.

Table 4. Simultaneous Inter – Area Transmission Transfer Efficiency of Nigerian grid

| **Simultaneous Inter - Area Transmission Transfers Efficiency (%)** | | | | | | | |
|---|---|---|---|---|---|---|---|
| **Sources/Sink Area** | | **Source Areas** | | | | | |
| | | **AREA 1&2** | **AREA 1&3** | **AREA 1&4** | **AREA 2&3** | **AREA 2&4** | **AREA 3&4** |
| **SINK AREAS** | **AREA 1** | Void | Void | Void | 94.53 | 95.17 | 91.68 |
| | **AREA 2** | Void | 97.07 | 95.52 | Void | Void | 97.24 |
| | **AREA 3** | 91.17 | Void | 98.99 | Void | 98.56 | Void |
| | **AREA 4** | 89.37 | 88.82 | Void | 95.23 | Void | Void |

The radial nature of the Nigerian 330kV transmission grid prompted the reason for tie line transmission performance. Outage of these lines could cause undue risk to part or the entire system with black out or system collapse being the resulting effects.

The performance of the tie line is obtained under different inter-area Available transfer capability. The receiving end power circle diagram, voltage profile and line load ability curves are equally obtained for a specified inter-area power transfer which is the specified receiving end quantities.

Table 5 gives the total receiving area load $P_{L(\lambda max)}^{RA}$ of inter-area Available Transfer Capability of Nigerian 330kV grid. All receiving area loads are assumed to be at 0.9 PF lagging. For each transfer case in Table 5, we determine the tie line performance. The tie line performance analysis is carried out in respect to each of the following,

- ✓ To calculate sending end quantities for specified receiving end MW and MVAR
- ✓ Obtain the receiving end power circle diagram
- ✓ Obtain load ability curve and voltage profile

At a power factor of 0.9 lagging, the Mvar at the receiving end are obtained and given in Table 6.

Figure 9 gives the receiving end power circle diagram with fixed sending $V_s$ end and varying receiving $V_r$ end voltages. $V_r$ varies from $V_r$ to 1.3 $V_r$. The tie line voltage variation in practice is allowed up to $1.1V_r$.

Table 7 gives the line performance quantities obtained for specified receiving end MW and MVar. Observe that the inter-area ATC from area1 to area2 results in higher transmission loss

and hence unacceptably high percentage voltage regulation. Series and shunt capacitors can be used to compensate the line in other to improve the line performance. It should be noted that Table 3 gives the network response ATTE values due to inter-area transfers; Table 7 presents the rated system path for transfer from area 1 to area 2. Hence, the network response method of ATTE provides somewhat too optimistic transfer efficiency as compared to the rated system path method. As shown in Figure 10, it is observe that while Transmission efficiency decreases with increase in real power loss, percentage voltage regulation increases with increase in real power loss both resulting from inter-area power transfer.

Table 5. Real Power Load (in MW) at the receiving area of Inter-area Transfer of Nigerian 330kV Grid

| Source/Sink Area | | SOURCE AREAS | | | |
|---|---|---|---|---|---|
| | | **AREA 1** | **AREA 2** | **AREA 3** | **AREA 4** |
| **SINK AREAS** | **AREA 1** | void | 881.41 | 1046.06 | 823.42 |
| | **AREA 2** | 1486.93 | void | 1578.79 | 1372.51 |
| | **AREA 3** | 450.00 | 333.28 | void | 336.59 |
| | **AREA 4** | 606.49 | 495.79 | 801.36 | void |

Table 6. Reactive Power Load (in Mvar) at the receiving area of Inter-area Transfer of Nigerian 330kV Grid

| Source/Sink Area | | SOURCE AREAS | | | |
|---|---|---|---|---|---|
| | | **AREA 1** | **AREA 2** | **AREA 3** | **AREA 4** |
| **SINK AREAS** | **AREA 1** | void | 426.87 | 506.61 | 398.78 |
| | **AREA 2** | 720.12 | void | 764.61 | 664.71 |
| | **AREA 3** | 217.93 | 161.41 | void | 163.01 |
| | **AREA 4** | 293.72 | 240.11 | 388.10 | void |

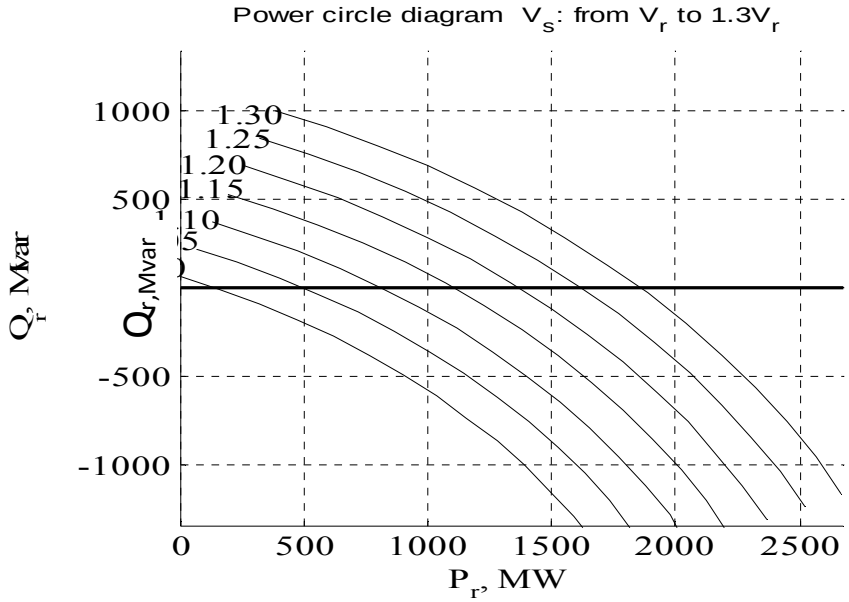


Figure 9. Power circle diagram of tie line connecting area1 to area2

Table 7. Tie line performance for specified receiving end ATC (Pr)

| Transfer | Vr (Volts) | Vs (Volts) | Required Sending ANGLE | Pr (MW) | Ps (MW) | Ploss (MW) | Is (A) | Ir(A) | % Voltage Regulation | Efficiency (%) |
|---|---|---|---|---|---|---|---|---|---|---|
| **Area1 TO Area2** | 330 | 458.43 | -25.84 | 1486.93 | 1784.61 | **297.68** | 2759.91 | 2890.48 | **41.23** | **83.32** |
| **Area1 To Area3** | 330 | 362.72 | 5.52 | 450.00 | 475.59 | **25.59** | 793.12 | 874.62 | **11.74** | **94.62** |
| **Area1 To Area4** | 330 | 376.56 | 7.05 | 606.49 | 654.01 | **47.52** | 1086.23 | 1178.97 | **16.00** | **92.73** |
| **Area2 To Area1** | 330 | 401.46 | 9.49 | 881.41 | 983.94 | **102.53** | 1606.64 | 1713.40 | **23.67** | **89.58** |
| **Area3 To Area1** | 330 | 416.69 | 10.81 | 1046.06 | 1191.57 | **145.51** | 1919.69 | 2033.46 | **28.37** | **87.78** |
| **Area4 To Area1** | 330 | 396.15 | 9.00 | 823.42 | 912.59 | **89.17** | 1496.56 | 1600.66 | **22.04** | **90.23** |

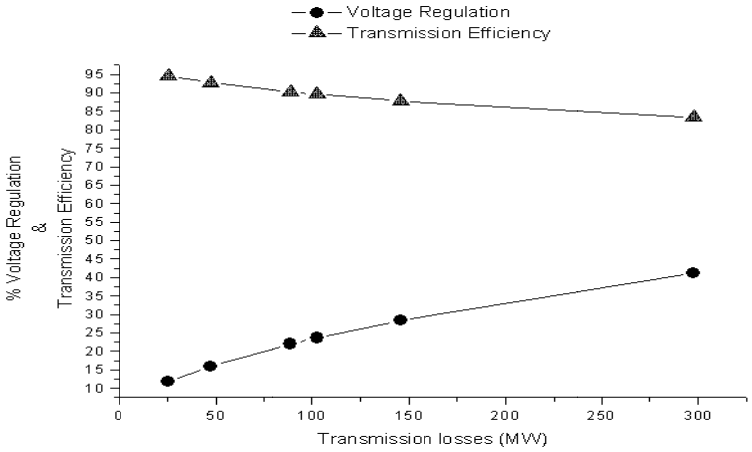


Figure 10. Transmission Real power loss with respect to voltage regulation and efficiency

Figure 11 shows the voltage profile for length up to one eight of wavelength under various scenarios of no load, surge impedance level (SIL), short circuit condition and rated load conditions.

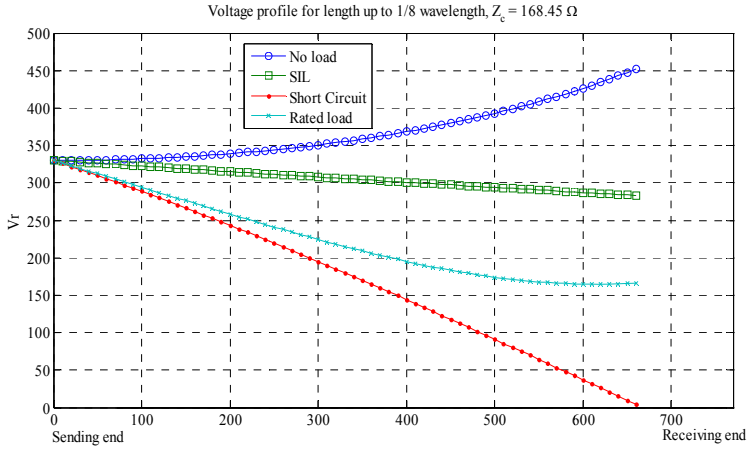


Figure 11. Voltage profile of the tie line under various loading condition

Figure 4 shows the tie line load ability curve under three limits: practical line load ability, theoretical stability limit and the thermal limit, all for up to one fourth of the wavelength. SIL obtained is 659.39MW at $30^0$.

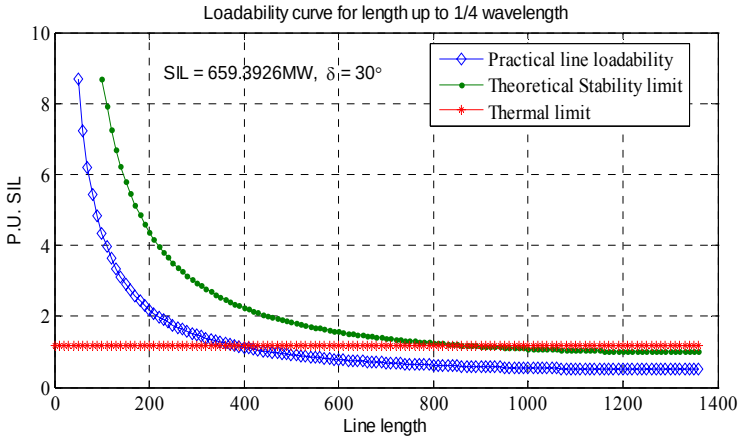


Figure 12. Tie line load ability curve for Area 1 TO Area 2 Transfer (Jebba TS to Oshogbo)

## 5. Conclusion

This paper used HCR-PF to compute inter-area available transfer capability (ATC) and presented a novel method for transmission transfer efficiency determination. Available Transmission Transfer efficiency (ATTE) uses ATC index to measure the performance of a tie line thereby taking into account the real power line losses. A plot of reactive power against the real power real power at the receiving end gives the power circle diagram. It is observed that while Transmission efficiency decreases with increase in real power loss, percentage voltage regulation increases with increase in real power loss both resulting from inter-area power transfer. It is therefore concluded that system wide (Network response) percentage efficiency values (as shown in table 3) is rather optimistic as compared with the tie line (Rated system path) performance (as indicated in table 7).

## 6. References

[1] Marannino, P., Bresesti, P., Garavaglia, A., Zanellini, F., & Vailati, R. (2002). *Assessing The Transmission Transfer Capability Sensitivity to Power System Parameters*. 14th PSCC, (pp. 1-7). Sevilla.

[2] NERC. (1996). Available Transfer Capability Definitions and Determination. Newyork: *North American Electric Reliability Council*.

[3] Omar, H. A., Masoud, A.-T., Mohammed, A.-w., Khalfan, A.-Q., Saqar, A.-F., Ibrahim, A.-B., et al. (2009). *Key Performance Indicators of A Transmission System. Sultanate of Oman: Oman Electricity Transmission Company*.

[4] Abu Dhabi Transmission and Dispatch Company TRANSCO. (2011). *Electricity Networks Annual Technical Report. Abu Dhabi*.

[5] Labo, H. S. (2010). Investors Forum For The Privatisation Of PHCN Successor Companies. Abuja: *Transmission Company of Nigeria*.

[6] Sauer, P. W. (1997). Technical Challenges of Computing Available Transfer Capability (ATC) in *Electric Power Systems. 30th Annual Hawaii International Conference on System Sciences. Hawaii*: PSerc: 97-04.

[7] Onahaebe, O., & Apeh, S. (2007). Voltage Instability in Electrical Network: A case study of Nigerian 330kV Transmission Grid. *Research Journal of Applied Sciences* 2 (8), 865 - 874.

[8] Sadiq, A., & Nwohu, M. (2013). Evaluation of Inter- Area Transfer Capability of Nigerian 330kV Network. *International Journal Engineering and Technology* Vol. 3 No. 2, 148-158.

[9] Hamoud, G. (2000). Feasibility Assessment of simultaneous bilateral transaction in a deregulated environmenr. *IEEE Transaction on power system*, 15 (1):22-6.

[10] Liu, C.-C., & Li, G. (2004). Available Transfer Capability Determination. Abuja: Third NSF Workshop on US-Africa Research and Education Collaboration.

[11] Yan, O., & Chanan, S. (2002). Assessment of Available Transfer Capability and Margins. *IEEE Transaction on Power systems*, vol. 17, no. 2, 463-468.

[12] Mark, H. G., & Chika, N. (1999). Available Transfer Capability and First order Sensitivity. *IEEE Transaction on Power System*, 512-518.

[13] Babulal, C., & Kannan, P. (2006). A Novel Approach for ATC Computation in *Deregulated Environment. J. Electrical Systems* 2-3, 146-161.

[14] Venkataramana, A., & Colin, C. (1992). The Continuation Power Flow: A Tool for Steady State Voltgae Stability Analysis. *IEEE Transactions Power System*, 416-423.

[15] Ejebe, G., Tong, J., Waight, J., Frame, J., Wang, X., & Tinney, W. (1998). Available Transfer Capability Calculations. *IEEE Transaction on Power Systems*, Vol. 13, No. 4, 1521-1527.

[16] Hsiao-Dong, C., Alexander, J. F., Kirit, S. S., & Neal, B. (1995). CPFLOW: A Practical Tool for Tracing Power System Steady-State Stationary Behavior Due to Load and Generation Variations. *IEEE Transaction on Power Systems*, Vol.10, No. 2, 623-633.

[17] Liang, M., & Ali, A. (2006). Total Transfer Capability Computation for Multi - Area Power Systems. *IEEE Transactions on Power Systems*, vol. 21, no. 3 , 1141-1147.

[18] Yuan-Kang, W. (2007). A novel algorithm for ATC calculations and applications in deregulated electricity markets. *Electrical Power and Energy Systems*, 810-821.

[19] Sadiq, A., Nwohu, M., & Ambafi, J. (2013). A Comparative Study on Implementation of Genetic Algorithm (GA) and ATC to Generator Sitting in Nigerian 330kV Network. *International Journal of Engineering Sciences.*

[20] Wu, T., & Fischl, R. (1993). An Algorithm for detecting the Contingencies which limit the inter-area megawatt Transfer. *North American Power Symposium*, (pp. 222-227). Washington D.C.

[21] Prabha, U., Venkataseshaiah, C., & Arumungam, S. M. (2010). Assessment of Available Transfer Capability incorporating Probabilistic Distriibution of Load Using Interval Arithmetic Method. *International Journal of Computer and Electrical Engineering*. Vol.2, No. 4, 692-697.

[22] Lubis, R. S., Hadi, S. P., & Tumiran. (2014). Using UPFC and GUPFC to Maximize Available Transfer Capability (ATC). *International Journal on Electrical Engineering and Informatics (IJEEI)*, 6 (2), 374-393.

[23] Saadat, H. (1999). Power System Analysis. In H. Saadat, Line Model and Performance New Delhi: Tata McGraw-Hill. pp. 142-164.

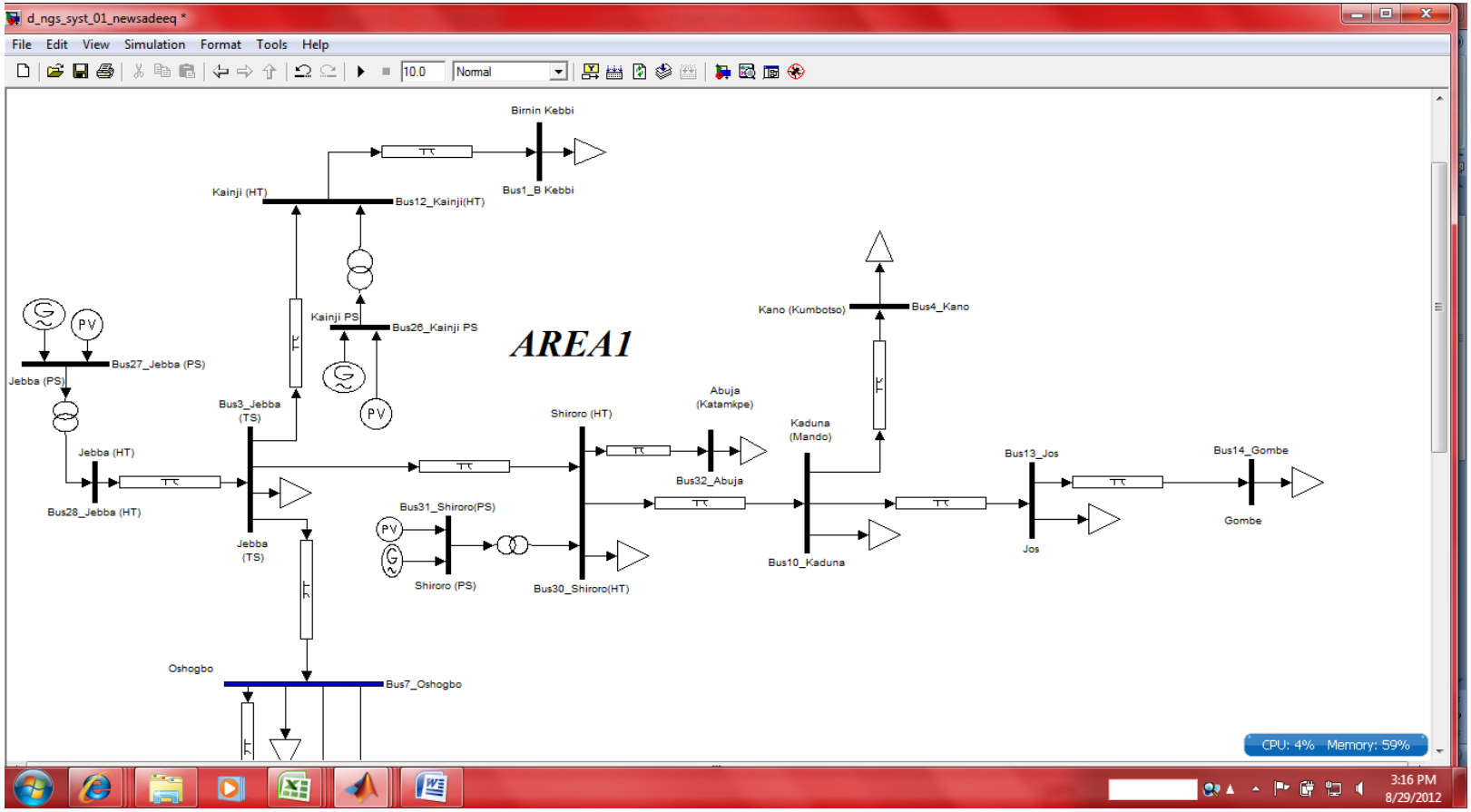
d_ngs_syst_01_newsadeeq *
File Edit View Simulation Format Tools Help
Normal
AREA1
Birnin Kebbi
Bus1_B Kebbi
Kainji (HT)
Bus12_Kainji(HT)
Kainji PS
Bus26_Kainji PS
Jebba (PS)
Bus27_Jebba (PS)
Bus3_Jebba (TS)
Jebba (HT)
Bus28_Jebba (HT)
Jebba (TS)
Bus31_Shiroro(PS)
Shiroro (PS)
Shiroro (HT)
Bus30_Shiroro(HT)
Abuja (Katamkpe)
Bus32_Abuja
Kano (Kumbotso)
Bus4_Kano
Kaduna (Mando)
Bus10_Kaduna
Bus13_Jos
Jos
Bus14_Gombe
Gombe
Oshogbo
Bus7_Oshogbo
CPU: 4% Memory: 59%
3:16 PM
8/29/2012

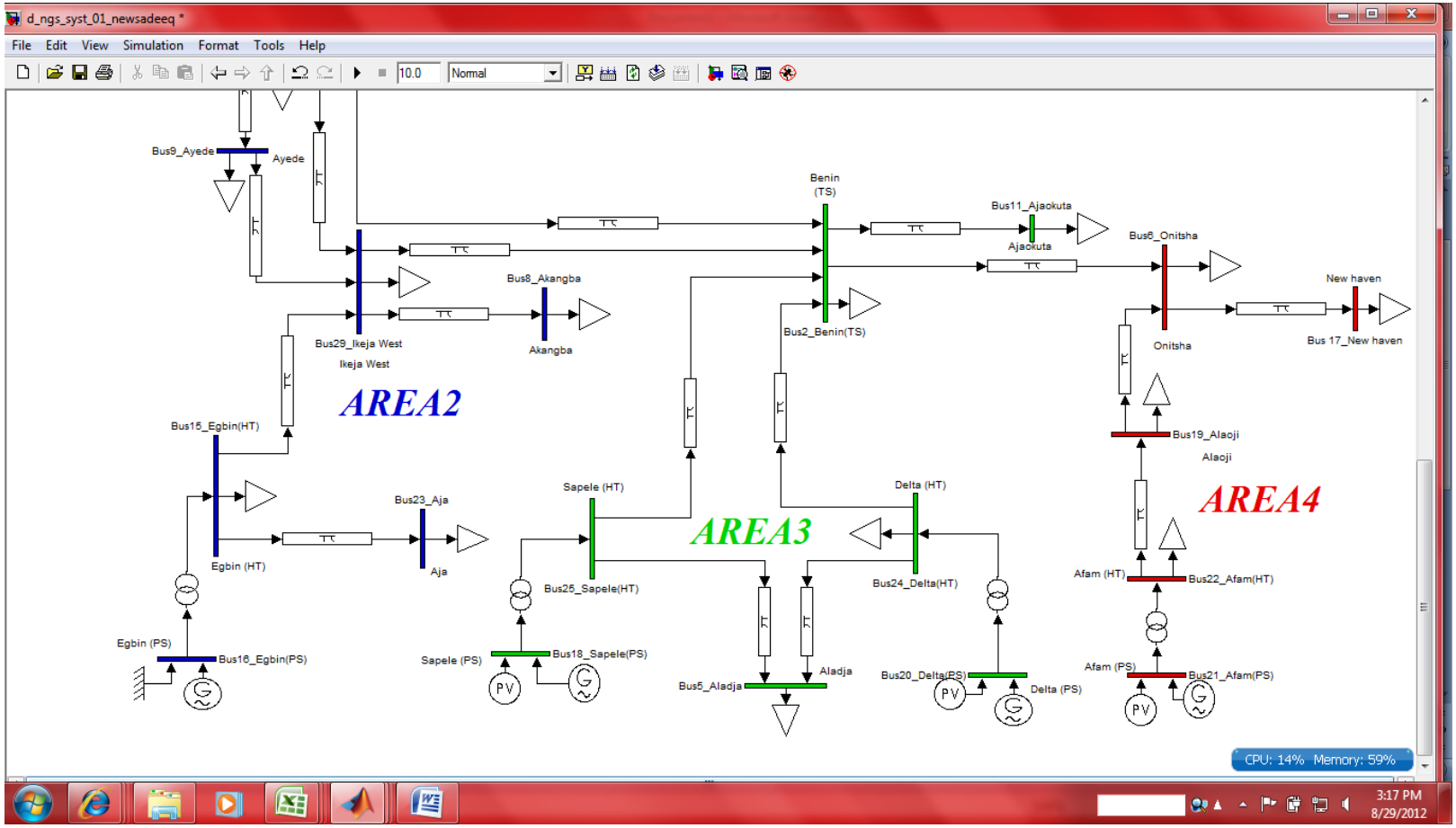
d_ngs_syst_01_newsadeeq *
File Edit View Simulation Format Tools Help
10.0
Normal
Bus9_Ayede
Ayede
Benin
(TS)
Bus11_Ajaokuta
Ajaokuta
Bus6_Onitsha
Bus8_Akangba
Akangba
New haven
Bus29_Ikeja West
Ikeja West
Bus2_Benin(TS)
Onitsha
Bus 17_New haven
AREA2
Bus15_Egbin(HT)
Bus19_Alaoji
Alaoji
Sapele (HT)
Delta (HT)
AREA4
Bus23_Aja
AREA3
Egbin (HT)
Aja
Bus25_Sapele(HT)
Bus24_Delta(HT)
Afam (HT)
Bus22_Afam(HT)
Egbin (PS)
Bus16_Egbin(PS)
Sapele (PS)
Bus18_Sapele(PS)
Aladja
Bus5_Aladja
Bus20_Delta(PS)
Delta (PS)
Afam (PS)
Bus21_Afam(PS)
PV
CPU: 14% Memory: 59%
3:17 PM
8/29/2012

**AHMAD, Abubakar Sadiq** was born im minna Nigeria on 29th July 1985. He received the B.Eng Degree in Electrical and Computer Engineering from Federal university of Technology, Minna Nigeria in 2008 and M.Eng in Electrical Power and Machines in 2013 from the same University. He is currently a Lecturer in the Department of Electrical and Electronics Engineering, Federal University of Technology, Minna. His research interest is in Power Systems Planning and Operations with specifics in Transfer capability assessment and Power Systems dynamics.

**NWOHU, Mark Ndubuka** was born in October 5, 1959 at Idiaraba Lagos State Nigeria. He received his bachelor of Engineering (B.Eng.) in Power Systems Engineering Technology from the Department of Electrical and Electronics Engineering, Federal University of Technology, Owerri, Nigeria, in 1988. He got his Masters degree in Power and Machines from the Electrical and Electronics Engineering Department, University of Benin, Nigeria in 1994. In 2007, he badged on his Doctor of Philosophy (PhD) Degree in Power Systems Engineering from Electrical and Electronics Engineering Programme, Abubakar Tafawa Balewa University, Bauchi, Nigeria. He is currently an Associate professor with the department of Electrical and Electronics Engineering, federal University of technology, Minna. His research interest includes Power System Analysis, Power System Stability and Control, Application of FACTS devices and Artificial Intelligence to Power Systems, System Simulation, Power Quality and Numerical Analysis.

**EUGENE, Okenna Agbachi** was born in Aku, Igbo-Etiti Local Government Area of Enugu, Nigeria. He obtained a Bachelor of Engineering (B. Eng) Degree, in Electrical and Computer Engineering Department, Federal University of Technology Minna in 2004 and a Master of Engineering (M. Eng; Power Devices Option) degree in Electrical Engineering from University of Nigeria Nsukka. He is currently pursuing the PhD degree in the Department of Electrical and Electronic Engineering of Federal University of Technology Minna, Nigerian. His research interest includes, Electric Power Devices and Hybrid Renewable Energy